Cureus
Part of SPRINGER NATURE

Open Access Original Article

Published via Contemporary Updates: Radiotherapy Innovation & Evidence (CURiE)

Comparative Cost-Effectiveness of Prostate-Specific Membrane Antigen Positron Emission Tomography Agents and Conventional Imaging for Initial Diagnosis of Prostate Cancer in the United States

Received 06/11/2026
Review began 07/01/2026
Review ended 09/24/2026
Published 11/01/2026

© Copyright 2026
Yee et al. This is an open access article distributed under the terms of the Creative Commons Attribution License CC-BY 4.0., which permits unrestricted use, distribution, and reproduction in any medium, provided the original author and source are credited.

DOI: 10.7759/cureus.118958

Christopher W. Yee [1], Yiqiao Xin [2], Mitchell Finkelstein [3], Steven E. Finkelstein [4], Christopher Tyson [5], Noam Kirson [1]

1. Health Economics and Outcomes Research, Analysis Group, Inc., Boston, USA 2. Health Economics and Outcomes Research, Analysis Group, Inc., London, GBR 3. Biomedical Sciences, Arizona State University, Tempe, USA 4. Radiation Oncology, US Urology Partners, Syracuse, USA 5. Health Economics and Outcomes Research (former employee), Lantheus Medical Imaging, Bedford, USA

Corresponding author: Christopher W. Yee, christopher.yee@analysisgroup.com

Abstract

Background: Molecular imaging with prostate-specific membrane antigen (PSMA)-targeted positron emission tomography (PET) radiotracers is more sensitive and specific than conventional imaging (CI) for both primary staging of prostate cancer and identifying biochemical recurrence. A recent cost-effectiveness analysis found that the PSMA PET tracer piflufolastat F 18 was more cost-effective compared to fluciclovine F-18, gallium68-PSMA-11 (PSMA 11), and CI (bone scans, computed tomography, and magnetic resonance imaging) for the diagnosis and staging of prostate cancer from a United States healthcare system perspective. With the 2023 approval of flotufolastat F 18 as a new PSMA PET tracer, we have updated the model to also assess its economic value.

Objective: The aim of this study was to assess the cost-effectiveness of piflufolastat F 18 in comparison to flotufolastat F 18, PSMA 11, and CI for the staging of prostate cancer in patients with newly diagnosed local or regional prostate cancer.

Methods: A hybrid economic model consisted of a decision tree to map out diagnosis and subsequent treatment, combined with a Markov model to predict the long-term outcomes of these treatment decisions, accounting for disease progression at initial imaging. Treatment pathways considered in the model included prostatectomy, radiation therapy, androgen deprivation therapy (ADT), radiotherapy + ADT, along with active surveillance. Model inputs were informed by data from clinical trials (OSPREY, CONDOR, LIGHTHOUSE), public data, and literature. Healthcare costs included diagnostic strategies, prostate cancer treatment, medical costs and adverse event (AE) management costs. Outcomes included life-years (LYs), quality-adjusted life-years (QALYs), and incremental cost-effectiveness ratio (ICERs).

Results: Over a lifetime horizon, piflufolastat F 18 had the greatest effectiveness in terms of LYs (6.79) and QALYs (5.23); for the comparators, LYs ranged from 6.51 (flotufolastat F 18) and 6.50 (CI) to 6.75 (PSMA 11) while QALYs ranged from 4.93 and 4.92 to 5.19, respectively. Compared to flotufolastat F 18, PSMA 11, and CI, piflufolastat F 18 was more cost-effective, having respective ICERs of $762, $91,985, and $138,434 per incremental QALY. Among the included imaging modalities, piflufolastat F 18 demonstrated the greatest net monetary benefit ($588,702) using a willingness-to-pay threshold (WTP) of $150,000. The key drivers included cost of diagnostics, test sensitivity, and probability of cure given treatment. At this WTP threshold, the probability that piflufolastat F 18 is cost-effective was 100.0%, 78.4%, and 71.0% compared to flotufolastat F 18, PSMA 11, and CI, respectively.

Conclusions: The findings of this analysis indicate that piflufolastat F 18 represents a cost-effective imaging modality for men with prostate cancer in the US. Compared with flotufolastat F 18, PSMA 11, and CI, piflufolastat F 18 was associated with higher projected LYs and QALYs, while generating a greater net monetary benefit.

Categories: Nuclear Medicine, Urology, Oncology
Keywords: cost-effectiveness analysis, cost-effectiveness model, economic evaluation, prostate cancer, prostate-specific membrane antigen, psma, psma pet

Introduction

Worldwide, prostate cancer is the most common cancer in men, accounting for approximately 15% of all male cancers, with the projected number of cases expected to reach 2.9 million by 2040 [1,2]. Prostate cancer

ranks as the second most commonly diagnosed malignancy and the second leading cause of cancer mortality among men in the United States (US), with an estimated 299,010 new cases and 35,250 deaths estimated in 2024 [3-5]. From birth to death, approximately 13% of all men in the US will develop prostate cancer at some point [5]. Although the five-year relative survival across prostate cancer stages is high (97%), the rate varies greatly for those with localized or regional disease (each associated with >99% survival) compared with distant (i.e., metastatic) disease (34%) [3]. Thus, clinical guidelines recommend screening for prostate cancer using both digital rectal exam and prostate-specific antigen (PSA) measurement, to promote early detection at less advanced stages [6-9].

The choice of first-line treatments for prostate cancer varies by disease stage and includes radical prostatectomy, radiotherapy, and, for patients at higher risk of progression, the addition of androgen deprivation therapy (ADT) [10]. However, up to 50% of patients receiving initial treatment with curative intent experience biochemical recurrence (BCR) within 10 years, which often precedes metastatic disease and is more difficult to treat [11-13]. Before initiating definitive local treatment, patients with unfavorable intermediate risk or higher who have suspected localized disease should undergo evaluation to rule out metastasis. Thus, once diagnosis is confirmed via biopsy [14], the extent of disease has historically been assessed using conventional imaging (CI) techniques such as computed tomography (CT), magnetic resonance imaging (MRI), bone scans, and/or positron emission tomography (PET) with the radiotracer 18F-fluorodeoxyglucose (18F-FDG) [15,16]. However, the poor sensitivity of CI modalities in detecting BCR and distant/metastatic disease has prompted interest in novel PET imaging methods with higher sensitivity and specificity [16-19]. With improvement in imaging techniques, the accuracy of prostate cancer staging and localization may increase, promoting better treatment decisions, earlier identification of progression, and improved patient outcomes [17]. For example, determining that PSA elevation comes from either a primary local recurrence or from metastatic spread can aid the identification of patients who could benefit from curative salvage radiotherapy [20-22]. On the other hand, failure to accurately stage disease, particularly at initial presentation, may result in higher expenditures for repeat testing along with less optimal treatment plans, leading to poorer survival outcomes and reduced quality of life.

The introduction of agents for the detection of prostate-specific membrane antigen (PSMA), the expression of which increases with higher prostate tumor grades, has revolutionized the diagnostic and prognostic applications of prostate cancer imaging [23-26]. Notably, PSMA-based PET tracers have been shown to be superior to CI for tumor localization, especially in the case of BCR or metastatic disease [19,27], and contribute more definitive findings and more frequent updates to disease management [28-31]. Accordingly, several novel PET agents have been approved by the US Food and Drug Administration (FDA) for men with prostate cancer who have suspected recurrence based on PSA level or suspected metastases [32]: fluciclovine F 18 (Axumin; Blue Earth Diagnostics, Needham, MA, USA) in 2016, gallium68-PSMA-11 (PSMA 11) in 2020 (University of California, Los Angeles and University of California, San Francisco) and in 2021 (Illuccix® commercial kit; Telix Pharmaceuticals, Fishers, IN, USA), piflufolastat F 18 (Pylarify®, Lantheus Medical Imaging, Bedford, MA, USA) in 2021, and flotufolastat F 18 (Posluma®, Blue Earth Diagnostics) in 2023 [33-36]. Prostate cancer management guidelines recognize PSMA PET as a highly sensitive and specific imaging modality for the detection of metastatic disease [16,18,21,37].

More recently, the Prostate Cancer Working Group 4 (PCWG4) has updated its recommendations on how to characterize and manage prostate cancer in both clinical and research settings [38]. In many situations, PCWG4 is now highlighting the importance of PSMA-PET imaging for both clinical and research settings. For instance, standard baseline disease assessments should now include detailed information around all PSMA-positive loci in the patient including not only the prostate bed but also nodal, visceral, and bone assessments. PCWG4 also sets recommendations for use of PSMA-PET imaging for clinical trial entrance and treatment monitoring within the study; although this expansion of PSMA-PET within the research setting may not have direct impact on disease management more broadly, it may foretell a broadening of PSMA-PET use in the clinical setting.

Given the rapid evolution of clinical imaging for prostate cancer as well as the entry of new PET tracers, a detailed understanding of the clinical and economic value of their incorporation into disease management plans is of interest to healthcare payers and providers. A previous cost-effectiveness study compared piflufolastat F 18 to fluciclovine F-18, PSMA 11, and CI for the diagnosis and staging of prostate cancer in the US, and the results showed greater life years (LY), quality-adjusted LYs (QALYs), and greater net monetary benefit for piflufolastat F 18 versus comparators [39]. Data from the LIGHTHOUSE trial of flotufolastat F 18 have provided additional information on its sensitivity and specificity in detecting BCR in prostate cancer [40], which affords the opportunity to also examine its relative economic value. In light of this, the objective of the present study was to evaluate the cost-effectiveness of piflufolastat F 18 compared to flotufolastat F 18 for the staging of prostate cancer from the perspective of the US healthcare system.

Materials And Methods

Model structure

As in our previously published study [39], this cost-effectiveness analysis used a hybrid model structure that combined a decision tree structure and a Markov model. The decision tree outlined the diagnostic and

treatment pathways, stratified by PSA levels (⩽1.0 or >1.0), capturing the proportions of patients categorized as having local, regional, distant, or no disease, and incorporated the sensitivities and specificities of specific imaging modalities. The reason for the stratification of PSA levels is that the sensitivity and specificity of the different PSMA PET agents differed for patients having a PSA of ⩽1.0 vs. >1.0, and these model inputs were reported according to this same cutoff in the source publications. The treatment pathways were fed into the Markov model, which simulated the long-term outcomes of prostate cancer given different treatment strategies. The model population was a mix of commercial and Medicare payers, and the model perspective was that of US payers, over a lifetime horizon.

The model included two key time points: initial diagnosis and BCR. Model inputs were considered independently for each time point, which included the distribution of patients between PSA levels (i.e., >1.0 or ⩽1.0) and of patients between different disease states (i.e., local, regional, distant, no disease), along with detection rates and treatment effectiveness. This approach aligns with evidence that the diagnostic sensitivity and specificity of PSMA PET tracers vary based on PSA levels, disease states, and at initial diagnosis versus recurrence [41]. Piflufolastat F 18 was the reference point for the comparators in the model, which included flotufolastat F 18, PSMA 11, and CI (i.e., an equally weighted mix of MRI, bone scan, and CT). Each imaging modality was modeled for initial staging/diagnosis along with BCR. To account for transitions occurring within model cycles, the model used a half-cycle correction when estimating the proportional distribution of patients across disease states. An additional half-cycle correction was not required for costs and utilities, since these already accounted for the corrected proportions.

Decision tree

The decision tree component of the model represented clinical decision-making by initially categorizing patients by disease state, and then by PSA levels (> 1.0 or ⩽ 1.0) (Figure *1*). Test accuracy would be dependent on disease state and PSA levels, and probabilities for diagnostic outcomes were assigned accordingly. For example, for patients with localized prostate cancer, the model predicted how many test results correctly indicated localized disease (true positives) along with those that incorrectly indicated an absence of prostate cancer (false negatives). In the case of patients who had no prostate cancer, the decision tree predicted how many test results indicated no disease (true negatives) versus those that incorrectly indicated the presence of prostate cancer (false positives). Patients would be designated different treatment assignments depending on their test results, which could include radiation therapy, ADT, prostatectomy, and active surveillance. Patients who were incorrectly diagnosed based on a false positive or false negative test result were assigned to a treatment that would be appropriate for the assumed disease state, which would last 12 months (e.g., a patient who truly had distant disease but had a false negative result would be treated for regional disease; a patient who truly had regional disease but had a false negative test result would be treated for local disease). After this 12-month period of receiving an incorrect treatment, these patients would go on to receive treatment appropriate for their true disease state, assuming no need for additional imaging or associated diagnostic costs.

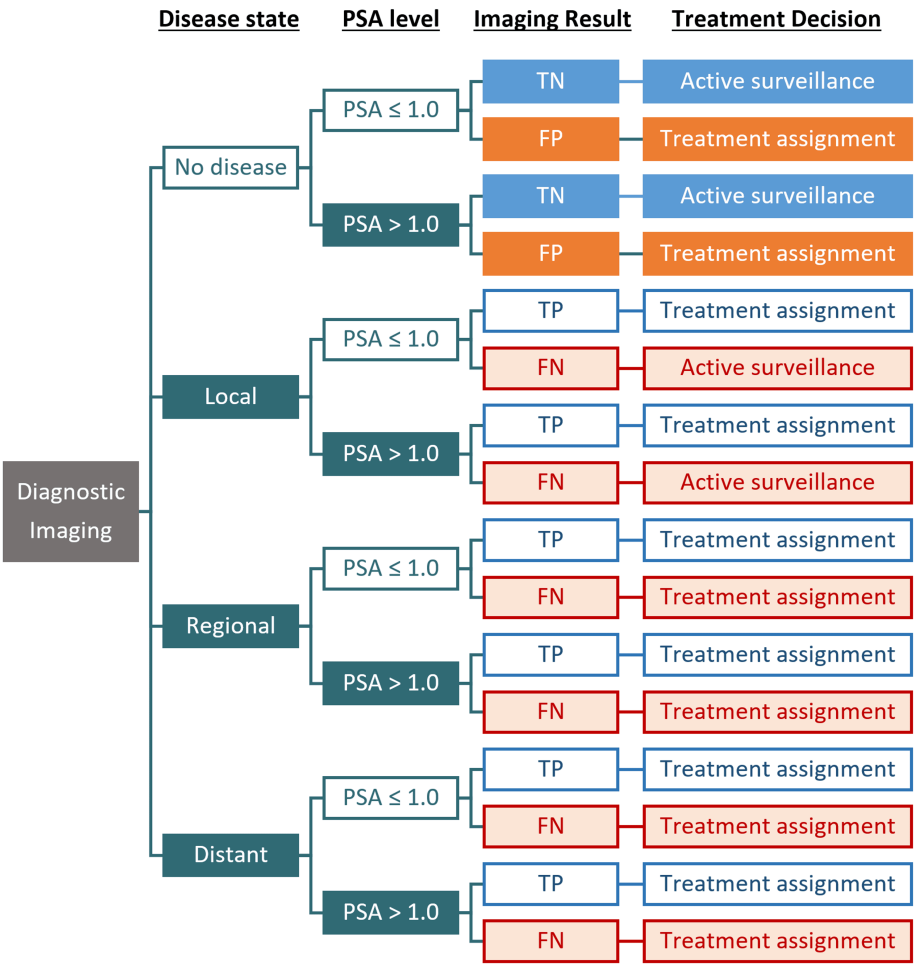


FIGURE 1: Decision tree (diagnosis pathway)

Abbreviations: FN, false negative; FP, false positive; PSA, prostate-specific antigen; TN, true negative; TP, true positive.

Figure reproduced from Yee et al., 2024 [39] under the CC BY-NC 4.0 license (http://creativecommons.org/licenses/by-nc/4.0/).

Markov model

The Markov model simulated how patients transitioned through various states of prostate cancer based on their treatment assignments following diagnosis (Figure *2*). Patients progressed through four different health states: (1) no prostate cancer (only applicable to recurrence diagnoses), (2) localized prostate cancer, (3) regional prostate cancer, and (4) distant prostate cancer. Transitions between these states were evaluated on a monthly basis, estimating the accumulated lifetime costs and clinical outcomes attributable to management of prostate cancer. Following a diagnosis of prostate cancer, patients received treatment aligned with the appropriate branch of the decision tree, which defined transitions between the health states of the Markov model starting from their initial health state. The transition probabilities were governed by the specific combinations of diagnostic pathways and treatment decisions from the decision tree component of the model. The model incorporated both prostate cancer-specific mortality and all-cause mortality.

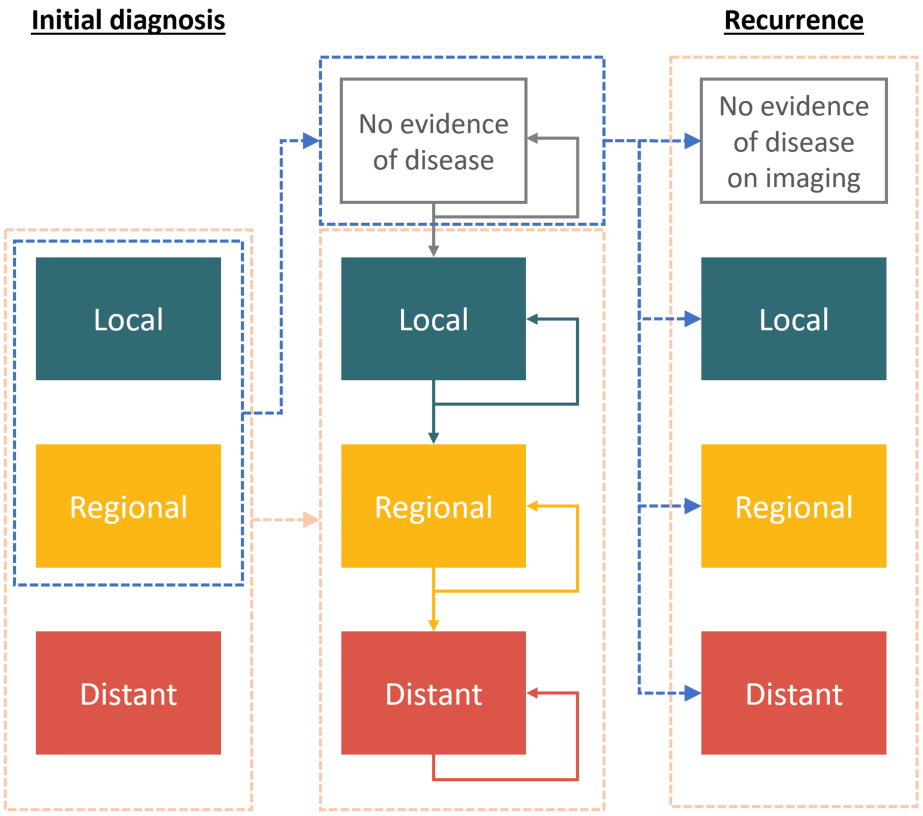


FIGURE 2: Markov model (disease progression)

Figure reproduced from Yee et al., 2024 [39] under the CC BY-NC 4.0 license (http://creativecommons.org/licenses/by-nc/4.0/).

Key assumptions

The model incorporated the following key assumptions: (1) It was assumed that the distribution of health states and PSA levels by disease state remained consistent regardless of the diagnostic method; (2) The sensitivity and specificity of each imaging modality were assumed to remain consistent across disease localization; (3) Patients were assumed to have treatment assignments purely based on imaging test results. For correct diagnoses (i.e., true positives and true negatives), the appropriate (i.e., corresponding to actual disease state) costs and QALYs were applied. For false negatives, where disease was present but undetected, the costs of treatment for a lower stage of disease were applied (i.e., assuming the patient was under-staged), while QALYs reflected the absence of appropriate treatment. For false positives, where disease was incorrectly diagnosed to be present, it was assumed that patients incurred unnecessary treatment costs and received no treatment benefit, and therefore the costs of treating local disease and QALYs for no disease were applied; (4) For incorrect diagnoses, the model assumed that patients received incorrect treatment for a period of 12 months; (5) Transitions in the Markov model were restricted to adjacent states (e.g., patients could not transition directly from localized to distant disease) due to a lack of supporting data for such transitions; (6) BCR was modeled as a one-time event, and the model did not explicitly account for performing repeat tests following an incorrect diagnosis; (7) Lastly, prostate cancer-specific mortality was modeled exclusively as a progression from the distant disease state.

Key model inputs

A targeted literature review was conducted to obtain model inputs, as previously described by Yee et al. [39], with the addition of search terms for the addition of flotufolastat F 18. In selecting data sources, preference was given to standalone clinical studies, particularly randomized controlled trials with larger sample sizes. Cost and utility inputs were preferentially selected from US-based studies to be consistent with the model setting and perspective. Claims-based studies were prioritized for healthcare cost inputs.

Clinical Parameters

Clinical parameters in the decision tree were informed by clinical trials and included disease state probabilities, distribution by PSA level, and probability of treatment assignments stratified by disease state and time point (Table *1*). Probabilities for disease state and PSA level distributions were derived from clinical

study reports of the OSPREY and CONDOR clinical trials, which reported the baseline PSA levels for each cohort receiving piflufolastat F 18 [42,43]. The distribution of initial treatment strategies was informed by expert opinion obtained through interviews with clinicians (see Acknowledgements). At recurrence diagnosis, these distributions were derived from model parameters from a US-based economic analysis assessing PSMA PET in staging recurrent prostate cancer [44,45].

	Value	Source
Disease state distribution (%)		
Initial diagnosis		
No disease	0	OSPREY 2301[a] [42]
Local	74.2	OSPREY 2301[a] [42]
Regional	25.8	OSPREY 2301[a] [42]
Distant	0	OSPREY 2301[a] [42]
Recurrence diagnosis		
No evidence of disease on imaging	0	CONDOR 3301[a] [43]
Local	27	CONDOR 3301[a] [43]
Regional	30	CONDOR 3301[a] [43]
Distant	43	CONDOR 3301[a] [43]
PSA distribution (%)		
Initial diagnosis		
No disease – ≤1.0	0	OSPREY 2301[a] [42]
No disease – >1.0	100	OSPREY 2301[a] [42]
Local – ≤1.0	0	OSPREY 2301[a] [42]
Local – >1.0	100	OSPREY 2301[a] [42]
Regional – ≤1.0	0	OSPREY 2301[a] [42]
Regional – >1.0	100	OSPREY 2301[a] [42]
Distant – ≤1.0	0	OSPREY 2301[a] [42]
Distant – >1.0	100	OSPREY 2301[a] [42]
Recurrence diagnosis		
No disease – ≤1.0	75	CONDOR 3301[a] [43]
No disease – >1.0	25	CONDOR 3301[a] [43]
Local – ≤1.0	34.5	CONDOR 3301[a] [43]
Local – >1.0	65.5	CONDOR 3301[a] [43]
Regional – ≤1.0	42.9	CONDOR 3301[a] [43]
Regional – >1.0	57.1	CONDOR 3301[a] [43]
Distant – ≤1.0	20.8	CONDOR 3301[a] [43]
Distant – >1.0	79.2	CONDOR 3301[a] [43]
Treatment assignment (%)		

Initial diagnosis		
No disease – active surveillance	100	Expert opinion
Local – radiation therapy	45	Expert opinion
Local – prostatectomy	55	Expert opinion
Regional – radiation therapy + ADT	100	Expert opinion
Distant – ADT	100	Expert opinion
Recurrence diagnosis		
No evidence of disease on imaging – active surveillance	100	Assumption
Local – radiation therapy	30	Jensen 2020 [44]
Local – ADT	35	Jensen 2020 [44]
Local – prostatectomy	5	Jensen 2020 [44]
Local – cryotherapy	5	Jensen 2020 [44]
Local – radiation therapy + ADT	25	Jensen 2020 [44]
Regional - radiation therapy	20	Jensen 2020 [44]
Regional - ADT	45	Jensen 2020 [44]
Regional – cryotherapy	5	Jensen 2020 [44]
Regional – radiation therapy + ADT	30	Jensen 2020 [44]
Distant - radiation therapy	30	Jensen 2020 [44]
Distant - ADT	45	Jensen 2020 [44]
Distant – radiation therapy + ADT	25	Jensen 2020 [44]
Costs (USD)		
Piflufolastat F 18	$6,274.17	CMS & Micromedex RED BOOK[b] [46,47]
Flotufolastat F 18	$6,311.17	CMS & Micromedex RED BOOK[b] [46,47]
PSMA 11	$6,103.67	CMS & Micromedex RED BOOK[b] [46,47]
MRI	$516.64	CMS [46]
SPECT	$1,481.84	CMS [46]
CT	$258.70	CMS [46]

TABLE 1: Key model inputs in the decision tree for the base case and probabilistic sensitivity analyses

Costs are presented in 2023 USD. Abbreviations: ADT, androgen deprivation therapy; CMS, Centers for Medicare & Medicaid Services; CT, computed tomography; MRI, magnetic resonance imaging; PSMA, prostate-specific membrane antigen; SPECT, single-photon emission computerized tomography; USD, United States dollars. Note: [a] Data on file, Lantheus Medical Imaging (Bedford, MA, USA); [b] Costs listed for each radiotracer include a facility payment amount of $1,642.84 for PET, sourced from CMS, added to the average wholesale price of each radiotracer, sourced from Micromedex RED BOOK.

Clinical parameters in the Markov model (Table *2*) included: probabilities of disease progression and adverse events (AEs), along with treatment efficacy, specifically the probability of curative treatment at each time point stratified by disease localization; along with transition probabilities benchmarked on European Randomized Study of Screening for Prostate Cancer (ERSPC) and Surveillance Epidemiology End Results (SEER) data, derived from previous models focused on prostate cancer [48-52]. AE rates associated with radiation therapy and prostatectomy were sourced from a US payer-perspective cost-utility evaluation of treatments for localized prostate cancer [53]. Estimates for cryotherapy-related AEs were derived from published meta-analyses and a population-based investigation of men with localized prostate cancer identified within a SEER-linked dataset [54-56]. Effectiveness estimates for radiation therapy, with and

without ADT, were informed by a retrospective cohort analysis of salvage treatment strategies after prostatectomy [57]. The effectiveness of ADT and cryotherapy was obtained from a propensity score-matched comparative study of patients treated with these interventions [58]. Effectiveness estimates for prostatectomy were based on a multicenter investigation of patients with recurrent disease after radiotherapy who underwent salvage radical prostatectomy [59]. Expert opinions, gathered through clinician interviews, informed probabilities for cure at initial diagnosis and the risk of recurrence following initial treatment.

	Value	Source
State transition probabilities (%)		
No disease to local (initial diagnosis)	9.7	Draisma 2003 [51]
No disease to local (recurrence diagnosis)	5.6	Cowen 1994 [48]
Local to regional	12.7	Cowen 1994 [48]
Regional to distant	34	Cowen 1994 [48]
Distant to death (prostate cancer-related)	26	Cowen 1994 [48]
Probabilities of adverse events (%)		
Erectile dysfunction in radiation therapy	27	Cooperberg 2013 [53]
Erectile dysfunction in ADT	10	Sciarra 2016 [54]
Erectile dysfunction in prostatectomy	42	Cooperberg 2013 [53]
Erectile dysfunction in cryotherapy	27	Zhou 2019 [55]
Erectile dysfunction in radiation therapy + ADT	27	Cooperberg 2013 [53]
Urinary incontinence in prostatectomy	9	Cooperberg 2013 [53]
Urinary incontinence in cryotherapy	10	Roberts 2011 [56]
Treatment effectiveness on transition probabilities (%)		
Local to regional		
Active surveillance	1	Assumption
Radiation therapy	0.27	Trock 2008 [57]
ADT	0.37	Bauman 2020 [58]
Prostatectomy	0.34	Chade 2011 [59]
Cryotherapy	0.31	Bauman 2020 [58]
Radiation therapy + ADT	0.36	Trock 2008 [57]
Regional to distant		
Active surveillance	1	Assumption
Radiation therapy	0.54	Trock 2008 [57]
ADT	0.64	Bauman 2020 [58]
Prostatectomy	0.61	Chade 2011 [59]
Cryotherapy	0.59	Bauman 2020 [58]
Radiation therapy + ADT	0.63	Trock 2008 [57]
Distant to death		
Active surveillance	1	Assumption
Radiation therapy	0.8	Trock 2008 [57]
ADT	0.86	Bauman 2020 [58]

Prostatectomy	0.84	Chade 2011 [59]
Cryotherapy	0.83	Bauman 2020 [58]
Radiation therapy + ADT	0.85	Trock 2008 [57]
Costs (USD)		
Treatment costs		
Active surveillance (Year 1)	1,329.51	Jensen 2020 [44]
Active surveillance (Year ≥ 2)	822.56	Jensen 2020 [44]
Radiation therapy (Year 1)	2,426.32	Jensen 2020 [44]
Radiation therapy (Year ≥ 2)	413.07	Jensen 2020 [44]
ADT (Year 1)	1,492.47	Jensen 2020 [44]
ADT (Year ≥ 2)	990.42	Jensen 2020 [44]
Prostatectomy (Year 1)	11,049.93	Jensen 2020 [44]
Prostatectomy (Year ≥ 2)	0	Jensen 2020 [44]
Cryotherapy (Year 1)	6,540.70	Jensen 2020 [44]
Cryotherapy (Year ≥ 2)	0	Jensen 2020 [44]
Radiation therapy + ADT (Year 1)	3,172.50	Jensen 2020 [44]
Radiation therapy + ADT (Year ≥ 2)	587.63	Jensen 2020 [44]
AE costs		
Erectile dysfunction (Year 1)	162.42	Cooperberg 2013 [53]
Erectile dysfunction (Year ≥ 2)	58.08	Cooperberg 2013 [53]
Urinary incontinence (Year 1)	108.92	Cooperberg 2013 [53]
Urinary incontinence (Year ≥ 2)	65	Cooperberg 2013 [53]
Medical costs		
HRU (Local)	2,746.00	Appukkuttan 2020 [60], Tangirala 2019 [61]
HRU (Regional)	3,295.20	Appukkuttan 2020 [60], Tangirala 2019 [61]
HRU (Distant)	5,784.58	Appukkuttan 2020 [60], Tangirala 2019 [61]
Utilities		
No disease	0.9	Jiang 2021 [62]
Local disease	0.79	Stewart 2005 [63]
Regional disease	0.67	Stewart 2005 [63]
Distant disease	0.25	Stewart 2005 [63]
Death (prostate cancer-related)	0	Assumption
Death (other causes)	0	Assumption
Erectile dysfunction	-0.1	Cooperberg 2013 [53]
Urinary incontinence	-0.2	Cooperberg 2013 [53]
Incorrect diagnosis period		
Incorrect diagnosis period (months)	12	Assumption
Probabilities of cure after initial diagnosis (%)		
Active surveillance in all states	0	Expert opinion
All active treatment for local disease	90	Expert opinion

All active treatment for regional disease	80	Expert opinion
All active treatment for distant disease	0	Expert opinion
Probabilities of recurrence from cure of initial disease		
Recurrence from cure of initial local disease	6.89	Expert opinion
Recurrence from cure of initial regional disease	16.74	Expert opinion

TABLE 2: Key model inputs in the Markov model for the base case and probabilistic sensitivity analyses

Costs are presented in 2023 USD. Abbreviations: ADT, androgen deprivation therapy; AE, adverse event; HRU, healthcare resource utilization; USD, United States dollars.

Diagnostic accuracy parameters used in the model, including PSA-stratified sensitivity and specificity estimates (PSA ⩽ 1.0 vs. > 1.0 ng/mL), are presented in Table 3. Performance estimates for piflufolastat F 18 were sourced from clinical documentation associated with the OSPREY trial [42], whereas values for flotufolastat F 18 were taken from clinical reports generated for the LIGHTHOUSE study [64]. Sensitivity estimates for PSMA 11 and CT were informed by a retrospective audit conducted at a single institution that evaluated gallium-68 PSMA PET/CT relative to conventional CT among patients with rising PSA levels following treatment [65]. Sensitivity inputs for single-photon emission computerized tomography (SPECT) were obtained from a retrospective single-center comparison of SPECT and F 18-choline PET/CT in patients originally referred for F 18-choline PET/CT imaging [66]. For PSA levels exceeding 1.0 ng/mL, specificity estimates for PSMA 11 and MRI were derived from a study evaluating gallium-68 PSMA-617 PET/CT alongside MRI in individuals with suspected prostate cancer [67]. MRI sensitivity was assumed to be equivalent to that of CT for PSA levels ⩽ 1.0 ng/mL and 5 percentage points higher than CT for PSA levels > 1.0 ng/mL. For PSA levels ⩽ 1.0 ng/mL, the specificity values for PSMA 11, MRI, SPECT, and CT for PSA ⩽ 1.0 were assumed to match that of fluciclovine F 18, based on the FALCON clinical trial and BED-001 study [68,69].

	%	Source
Piflufolastat F 18		
Sensitivity - PSA ≤ 1.0	57	OSPREY 2301[a] [42]
Sensitivity - PSA > 1.0	97	OSPREY 2301[a] [42]
Specificity - PSA ≤ 1.0	93	OSPREY 2301[a] [42]
Specificity - PSA > 1.0	55	OSPREY 2301[a] [42]
Flotufolastat F 18		
Sensitivity - PSA ≤ 1.0	24	LIGHTHOUSE [40]
Sensitivity - PSA > 1.0	24	LIGHTHOUSE [40]
Specificity - PSA ≤ 1.0	96	LIGHTHOUSE [40]
Specificity - PSA > 1.0	96	LIGHTHOUSE [40]
PSMA 11		
Sensitivity - PSA ≤ 1.0	41	Asokendaran 2019 [65]
Sensitivity - PSA > 1.0	92	Asokendaran 2019 [65]
Specificity - PSA ≤ 1.0	67	Expert opinion (same as fluciclovine F 18)
Specificity - PSA > 1.0	89	Li 2020 [67]
MRI		
Sensitivity - PSA ≤ 1.0	18	Expert opinion (same as CT)
Sensitivity - PSA > 1.0	68	Expert opinion (+5% above CT)
Specificity - PSA ≤ 1.0	67	Expert opinion (same as fluciclovine F 18)
Specificity - PSA > 1.0	53	Li 2020 [67]
SPECT		
Sensitivity - PSA ≤ 1.0	10	de Leiris 2020 [66]
Sensitivity - PSA > 1.0	25	de Leiris 2020 [66]
Specificity - PSA ≤ 1.0	67	Expert opinion (same as fluciclovine F 18)
Specificity - PSA > 1.0	31	Expert opinion (same as fluciclovine F 18)
CT		
Sensitivity - PSA ≤ 1.0	18	Asokendaran 2019 [65]
Sensitivity - PSA > 1.0	63	Asokendaran 2019 [65]
Specificity - PSA ≤ 1.0	67	Expert opinion (same as fluciclovine F 18)
Specificity - PSA > 1.0	31	Expert opinion (same as fluciclovine F 18)

TABLE 3: Test performance inputs in populations with different PSA levels

Abbreviations: CT, computed tomography; MRI, magnetic resonance imaging; PSMA, prostate-specific membrane antigen; PSA, prostate-specific antigen; SPECT, single-photon emission computerized tomography. Note: [a] Data on file, Lantheus Medical Imaging (Bedford, MA, USA).

Healthcare Costs

Costs were incorporated to capture the range of imaging modalities captured in the decision tree (i.e., piflufolastat F 18, flotufolastat F 18, PSMA 11, MRI, SPECT, and CT), treatments, and management of AEs

(Tables 1, 2). Cost inputs for imaging procedures were derived via Physician Fee Schedule values from the Centers for Medicare & Medicaid Services (CMS) and Micromedex RED BOOK [46,47]. Cost inputs for prostate cancer treatment were based on a previous economic model of PSMA PET imaging of recurrent prostate cancer in the US [44,70]. Costs related to the management of erectile dysfunction and urinary incontinence were derived from a US payer-perspective cost-utility study evaluating treatment options for localized prostate cancer [53]. Other medical costs (i.e., healthcare resource utilization specific to disease state) were based on hospital-based US claims studies [60,61]. All costs were reported in 2023 US dollars (USD), adjusted using the Consumer Price Index for medical care services [71] with a 3% annual discount, in accordance with guidance for US-based economic comparisons [72].

QALYs

Utilities, as well as disutilities related to AEs, were considered for each disease state in the Markov model in the estimation of QALYs. The baseline utility assigned to individuals without prostate cancer was derived from a US study reporting EQ-5D-5L population reference values; the median utility estimate (0.90) for subjects aged 65-74 years was selected because this age group closely corresponded with the typical age when prostate cancer is diagnosed (67 years) [3,62]. Utility estimates for local, regional, and metastatic disease states were obtained from a study of US men aged 60 years or older, of whom 52% had been diagnosed with prostate cancer [63]. Disutilities associated with erectile dysfunction and urinary incontinence were sourced from a US payer-perspective cost-utility evaluation of treatment strategies for localized prostate cancer [53,73]. Death, whether due to prostate cancer or other causes, was assigned a utility value of zero. An annual discount rate of 3% was applied [72].

Analyses

For each imaging modality, the analyses evaluated total healthcare costs, LY, and QALYs. Incremental cost-effectiveness ratios (ICERs) were derived by calculating the additional cost associated with one strategy relative to another and dividing this value by the incremental QALYs gained. An imaging modality was considered cost-effective when its ICER fell below the upper threshold commonly used by the Institute for Clinical and Economic Review as a benchmark for health-benefit pricing, a willingness-to-pay (WTP) threshold of $150,000 USD per QALY [74]. Net monetary benefit (NMB) was calculated for each strategy by multiplying the total QALYs gained by the WTP threshold and then subtracting the associated total costs.

Deterministic Sensitivity Analysis (DSA)

In addition to the base case analyses, DSAs were conducted to examine how uncertainty in influential model inputs affected the model outputs. The parameters varied in these analyses included the initial PSA distribution across disease states, the sensitivity and specificity of diagnostic tests, the costs associated with diagnostics, the distribution of disease across stages/localizations (i.e., local, regional, and distant), health state utility values, and the probability of having curative treatment at the time of initial diagnosis. Each parameter was systematically varied within the range defined by its lower and upper 95% confidence interval. These confidence intervals were derived from the parametric distributions used in the probabilistic sensitivity analyses, ensuring consistency in the interpretation of uncertainty. By varying these parameters individually, the DSA provided insights into which factors exerted the greatest influence on the model's outcomes, thereby identifying key drivers of cost-effectiveness.

Probabilistic Sensitivity Analysis

To account for uncertainty across multiple parameters simultaneously, probabilistic sensitivity analyses were conducted. This approach involved assigning appropriate probability distributions to different types of parameters based on their characteristics. Beta distributions were applied to binary variables, such as diagnostic test performance (sensitivity and specificity), health state utility values, transition probabilities, and probabilities of curative treatment. Gamma distributions were used for cost-related parameters, while Dirichlet distributions were assigned to the true disease state distributions, reflecting the probabilities of mutually exclusive outcomes. The sources and values of the parameters used in the probabilistic sensitivity analysis are listed in Table 4.

Parameters	Base case value	Distribution in probability sensitivity analysis	Standard error	Alpha	Beta
Disease state distribution at recurrence (%)[43]					
Local	0.27	Dirichlet	-	31.59	-
Regional	0.3	Dirichlet	-	35.1	-
Distant	0.43	Dirichlet	-	50.31	-
Disease state distribution at initial diagnosis (%)					

[42]					
Local	0.742	Dirichlet	-	186.98	-
Regional	0.258	Dirichlet	-	65.02	-
Test performance (%)[a]					
Piflufolastat F 18					
Sensitivity - PSA ≤ 1.0	0.57	Beta	0.06	11.44	36.22
Sensitivity - PSA > 1.0	0.97	Beta	0.06	11.44	36.22
Specificity - PSA ≤ 1.0	0.93	Beta	0.01	291.64	12.15
Specificity - PSA > 1.0	0.55	Beta	0.01	291.64	12.15
Flotufolastat F 18					
Sensitivity - PSA ≤ 1.0	0.24	Beta	0.05	30.81	71.89
Sensitivity - PSA > 1.0	0.24	Beta	0.13	5.82	1.03
Specificity - PSA ≤ 1.0	0.96	Beta	0.1	14	6.89
Specificity - PSA > 1.0	0.96	Beta	0.05	30.36	67.57
PSMA 11					
Sensitivity - PSA ≤ 1.0	0.41	Beta	0.06	28.7	41.3
Sensitivity - PSA > 1.0	0.92	Beta	0.03	71.76	6.24
Specificity - PSA ≤ 1.0	0.67	Beta	0.12	9.99	4.92
Specificity - PSA > 1.0	0.89	Beta	0.03	102.13	12.62
MRI					
Sensitivity - PSA ≤ 1.0	0.18	Beta	0.05	12.6	57.4
Sensitivity - PSA > 1.0	0.68	Beta	0.05	53.04	24.96
Specificity - PSA ≤ 1.0	0.67	Beta	0.12	9.99	4.92
Specificity – PSA > 1.0	0.53	Beta	0.14	6.64	5.89
SPECT					
Sensitivity - PSA ≤ 1.0	0.1	Beta	0.09	0.9	8.1
Sensitivity - PSA > 1.0	0.25	Beta	0.04	26	78
Specificity - PSA ≤ 1.0	0.67	Beta	0.12	9.99	4.92
Specificity - PSA > 1.0	0.31	Beta	0.13	3.72	8.28
CT					
Sensitivity - PSA ≤ 1.0	0.18	Beta	0.05	36.26	165.2
Sensitivity - PSA > 1.0	0.63	Beta	0.05	15.81	9.29
Specificity - PSA ≤ 1.0	0.67	Beta	0.12	14	6.89
Specificity - PSA > 1.0	0.31	Beta	0.13	30.36	67.57
Transition probabilities (%)[a]					
No Disease to Local (GS >7) at recurrence	0.056	Beta	0.01	41.9	706.31
No Disease to Local (GS >7) at initial diagnosis	0.097	Beta	0.01	40.04	372.71
Local (GS > 7) to Regional for both initial diagnosis and recurrence	0.127	Beta	0.02	38.67	265.84
Regional to Distant for both initial diagnosis and	0.34	Beta	0.05	28.99	56.28

recurrence					
Distant to Death (PCa related) for both initial diagnosis and recurrence	0.26	Beta	0.04	32.63	92.87
HRU[a]					
HRU (Local)	2746	Gamma	411.9	44.44	61.79
HRU (Regional)	3295	Gamma	494.28	44.44	74.14
HRU (Distant)	5785	Gamma	867.69	44.44	130.15
Utilities					
No disease [62]	0.9	Beta	0.01	1264.73	140.53
Local disease [63]	0.79	Beta	0.03	148.68	40.32
Regional disease [63]	0.67	Beta	0.04	117.63	57.94
Distant disease [63]	0.25	Beta	0.01	208.94	626.83
Erectile dysfunction [53]	-0.1	Beta	0.03	13.73	123.56
Urinary incontinence [53]	-0.2	Beta	0.05	12.09	48.37
Probability of cure[a]					
Radiation therapy - Local	0.9	Beta	0.14	3.54	0.39
Radiation therapy - Regional	0.8	Beta	0.12	8.09	2.02
ADT - Local	0.9	Beta	0.14	3.54	0.39
ADT - Regional	0.8	Beta	0.12	8.09	2.02
Prostatectomy - Local	0.9	Beta	0.14	3.54	0.39
Prostatectomy - Regional	0.8	Beta	0.12	8.09	2.02
Radiation therapy + ADT- Local	0.9	Beta	0.14	3.54	0.39
Radiation therapy + ADT - Regional	0.8	Beta	0.12	8.09	2.02
Recurrence Probabilities[a]					
Cure to recurrence given start in local	0.07	Beta	0.01	41.32	558.76
Cure to recurrence given start in regional	0.17	Beta	0.03	36.83	183.14

TABLE 4: Probabilistic sensitivity analysis inputs

[a] Variability of 15% was assumed

PSMA, prostate-specific membrane antigen; PSA, prostate-specific antigen; GS: Gleason Score; PCa: prostate cancer; HRU: healthcare resource utilization; SPECT, single-photon emission computerized tomography; ADT: androgen deprivation therapy

The probabilistic sensitivity analysis was conducted using 500 iterations, with the number of simulations determined by convergence plots that tracked the ICER of piflufolastat F 18 compared to flotufolastat F 18, PSMA 11, and CI. Parameter uncertainty was characterized using standard error (SE) or confidence intervals reported in literature where available, or SEs assumed to be equal to 15% of the mean if not otherwise reported.

Model validation

The methodology and reporting were developed in accordance with the Consolidated Health Economic Evaluation Reporting Standards (CHEERS) recommendations [75]. The model structure, assumptions, and results were validated by clinical experts (see Acknowledgements). To test the robustness of the model, extreme value testing was performed across multiple variable categories, which included: the distribution of disease states and PSA levels, diagnostic test sensitivity and specificity, probabilities of treatment decisions, diagnostic imaging costs, transition probabilities, AE rates and costs, treatment-effect estimates (hazard

rates), overall treatment costs, health state utility values, and probabilities of curative treatment. As an additional validation step, the core state-transition framework was independently programmed twice in Excel (Microsoft, Redmond, WA, USA) and the resulting implementations were cross-checked for consistency. Separate quality-control reviews of spreadsheet formulas and Visual Basic for Applications (VBA) code were conducted to identify potential computational, programming, or logical errors.

Results

Base case

When evaluated across the lifetime analytic horizon of the model, piflufolastat F 18 was found to be the most effective imaging option, resulting in 6.79 LYs and 5.23 QALYs (Table 5). PSMA 11 had the highest effectiveness among the comparators, with 6.75 LYs and 5.19 QALYs, while flotufolastat F 18 and SPECT had the lowest values, at 6.51 LYs and 4.93 QALYs, and 6.50 LYs and 4.92 QALYs, respectively.

Diagnostic options	Total			Incremental outcomes (piflufolastat F 18 vs. each comparator)			Combined outcomes		
	Cost ($)	LY	QALY	Δ Cost ($)	Δ LY	Δ QALY	ICER (Δ $/ Δ LY)	ICER (Δ $/ Δ QALY)	Net monetary benefit (threshold of $150,000)
Piflufolastat F 18	$195,101	6.79	5.225	-	-	-	-	-	$588,702
Comparators									
Flotufolastat F 18	$194,876	6.51	4.93	$226	0.2782	0.2958			
PSMA 11	$192,210	6.75	5.194	$2,891	0.0394	0.0314	$73,305	91,985	$586,878
CI (MRI, SPECT, CT equally weighted)	$167,447	6.58	5.026	$27,655	0.2034	0.1998	$135,967	138,434	$586,391

TABLE 5: Cost-effectiveness base case results

Costs are presented in 2023 United States dollars. Abbreviations: CT, computed tomography; ICER, incremental cost-effectiveness ratio; LY, life year; MRI, magnetic resonance imaging; PSMA, prostate-specific membrane antigen; QALY, quality-adjusted life year; CI, conventional imaging; SPECT, single-photon emission computerized tomography.

In terms of cost-effectiveness, piflufolastat F 18 had an ICER of $762/QALY gained vs. flotufolastat F 18, $91,985 per QALY gained vs. PSMA 11, and $138,434 per QALY gained vs. CI. This indicates that piflufolastat F 18 was the most cost-effective option versus these comparators, extensively dominating both PSMA 11 and flotufolastat F 18.

In addition, piflufolastat F 18 had the highest NMB ($588,702) compared to flotufolastat F 18 ($544,550), PSMA 11 ($586,878), and CI ($586,391) at a WTP threshold of $150,000, despite having the highest total cost.

DSA

The DSA identified several common drivers influencing the cost-effectiveness of piflufolastat F 18 across all comparator imaging strategies. These included diagnostic costs, test sensitivity, and the probability of achieving a cure given treatment. Other influential parameters differed depending on the comparator, as did their ranking in terms of importance. The influence of individual model drivers on the ICER differed by comparator; however, in most scenarios, the resulting ICERs remained below the WTP threshold of $150,000.

Piflufolastat F 18 Versus Flotufolastat F 18

Several scenarios showed conditions in which piflufolastat F 18 would dominate flotufolastat F 18. First, a 26% reduction in the cost of piflufolastat F 18 led to a negative incremental cost (-$6,921) while achieving higher QALYs gained (0.319) (Figure 3). Similarly, a 32% increase in the cost of flotufolastat F 18 would lead to a negative incremental cost (-$8,530) and an increase in the QALYs gained (0.319). Dominance was also observed with a decrease in the sensitivity of piflufolastat F 18 by 47% for PSA £ 1.0 (-$1,697 and 0.296 QALYs gained). Conversely, an increase in the sensitivity of flotufolastat F 18 by 42% for PSA £ 1.0 would lead it to be dominated by piflufolastat F 18 (-$51 and 0.311 QALYs gained). Additionally, a 23% reduction in the

proportion of patients with regional disease would lead piflufolastat F 18 to dominate flotufolastat F 18. Excluding scenarios in which piflufolastat F 18 dominated flotufolastat F 18, ICERs ranged from $579 to $32,414 per QALY gained. Because every estimate remained below the $150,000 WTP threshold, piflufolastat F 18 was considered cost-effective across all scenarios evaluated.

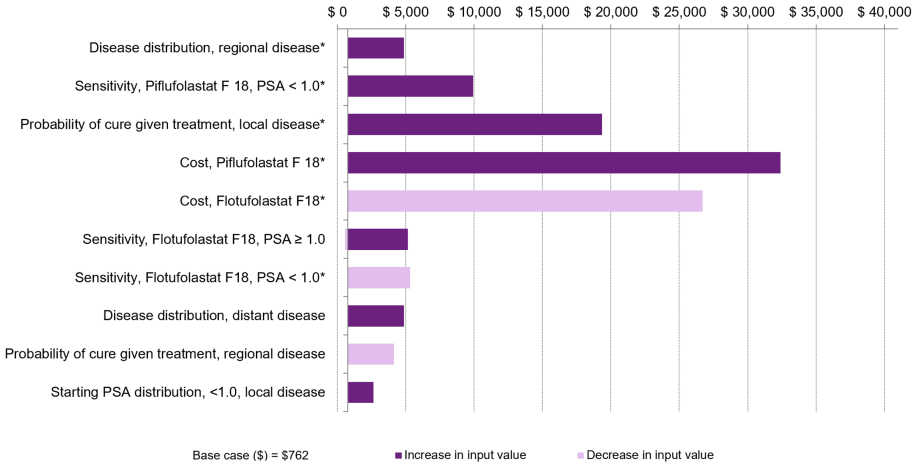


FIGURE 3: Deterministic sensitivity analysis - Piflufolastat F 18 versus Flotufolastat F 18

PSA, prostate-specific antigen.

Figure created by the authors using Microsoft Excel (Redmond, WA, USA).

Piflufolastat F 18 Versus PSMA 11

A similar pattern was observed in the comparison with PSMA 11, where piflufolastat F 18 became the dominant strategy under comparable cost assumptions. Specifically, decreasing the cost of piflufolastat F 18 by 26% or increasing the cost of PSMA 11 by 32% resulted in lower overall costs together with greater QALY gains (Figure *4*). Aside from imaging costs, the parameters with the greatest influence on this comparison were the sensitivity estimates for patients with PSA ⩾1.0. Reducing the sensitivity of piflufolastat F 18 by 4% increased the ICER to $134,156 per QALY, whereas increasing the sensitivity of PSMA 11 by 12% increased the ICER to $272,432 per QALY. Across all remaining scenarios, ICER estimates stayed below the WTP threshold of $150,000 per QALY, supporting the conclusion that piflufolastat F 18 remained a cost-effective alternative to PSMA 11.

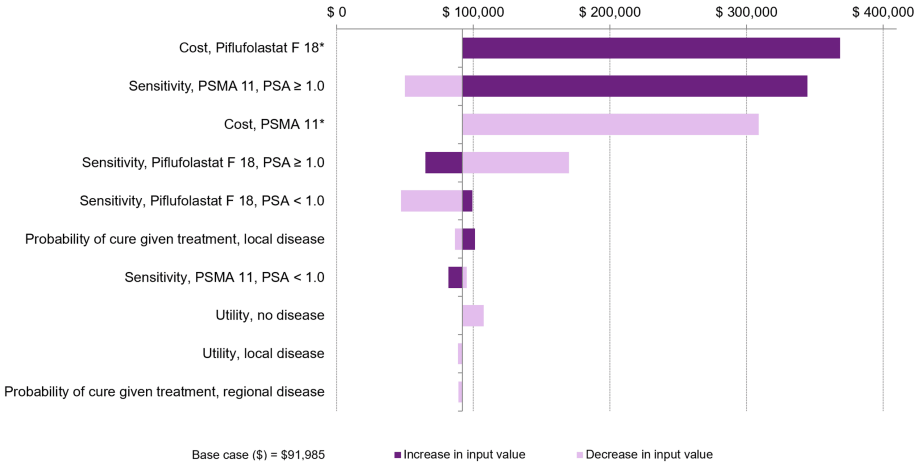


FIGURE 4: Deterministic sensitivity analysis - Piflufolastat F 18 versus PSMA 11

PSA, prostate-specific antigen; PSMA, prostate-specific membrane antigen.

Figure created by the authors using Microsoft Excel (Redmond, WA, USA).

Piflufolastat F 18 Versus CI

When piflufolastat F 18 was compared against CI, the cost of piflufolastat F 18 was the primary driver of the ICER (Figure 5). A 26% reduction in the cost of piflufolastat F 18 would decrease the ICER to $96,792, while a 32% increase in the cost would raise the ICER to $176,792. The sensitivity of CI for PSA ⩽ 1.0 was also influential, with a 50% reduction leading to a lower ICER of $110,636, while an increase of 50% would lead to a higher ICER of $164,600. The model was also sensitive to the utility value assigned to the “no disease” health state. When this was decreased from the base-case value of 0.9 down to 0.79, corresponding to the utility for localized prostate cancer, the ICER increased to $172,356 per QALY. Piflufolastat F 18 was not dominant over CI in any of the scenarios examined, and ICERs otherwise stayed below the WTP threshold of $150,000 per QALY, confirming its cost-effectiveness relative to CI.

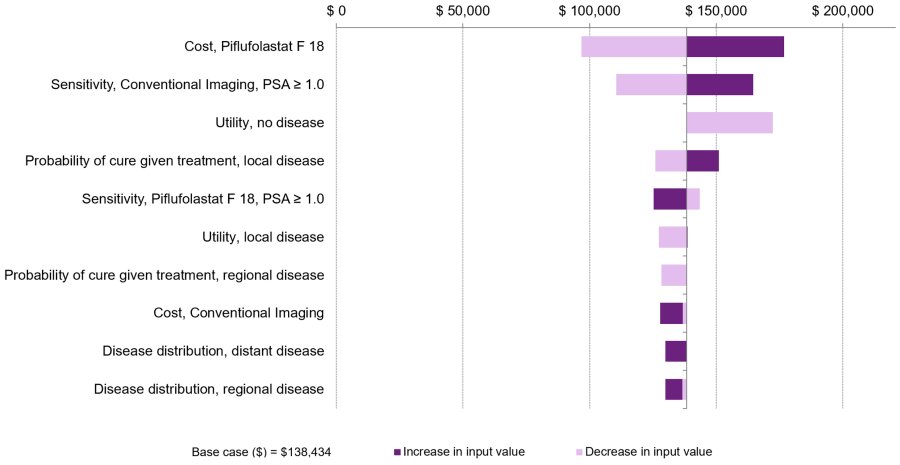


FIGURE 5: Deterministic sensitivity analysis - Piflufolastat F 18 versus Conventional Imaging

PSA, prostate-specific antigen.

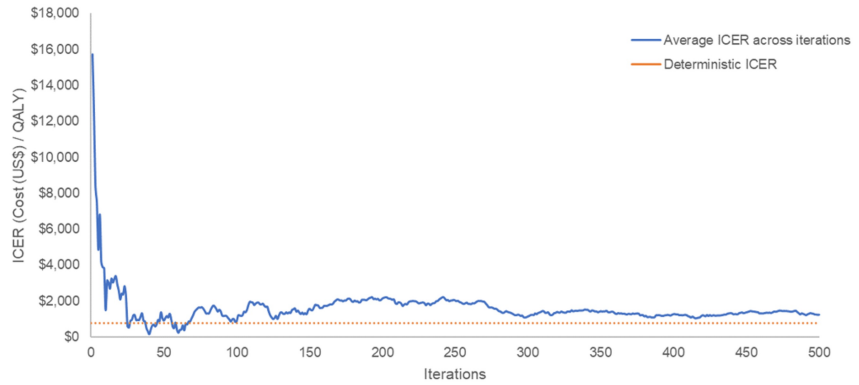
Figure created by the authors using Microsoft Excel (Redmond, WA, USA).

Probabilistic sensitivity analysis

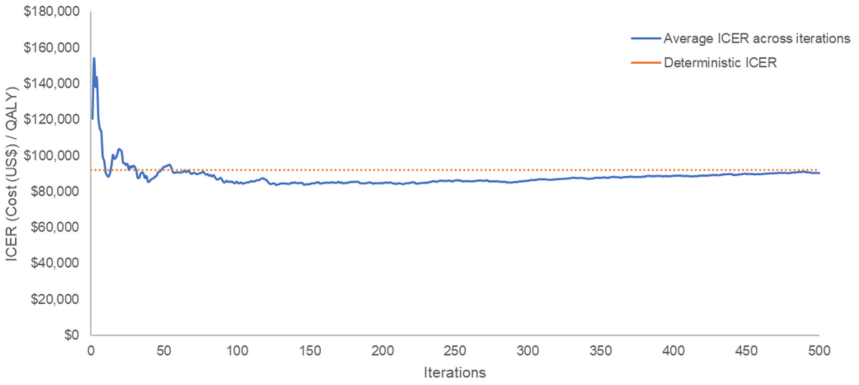
The probabilistic ICER achieved stability after approximately 300 simulations, as confirmed through visual

inspection of the ICER convergence plot (Figure 6). For the full probabilistic sensitivity analysis, a total of 500 simulations were run.

a. Piflufolastat F 18 vs. Flotufolastat F 18



b. Piflufolastat F 18 vs. PSMA 11



c. Piflufolastat F 18 vs. Conventional Imaging

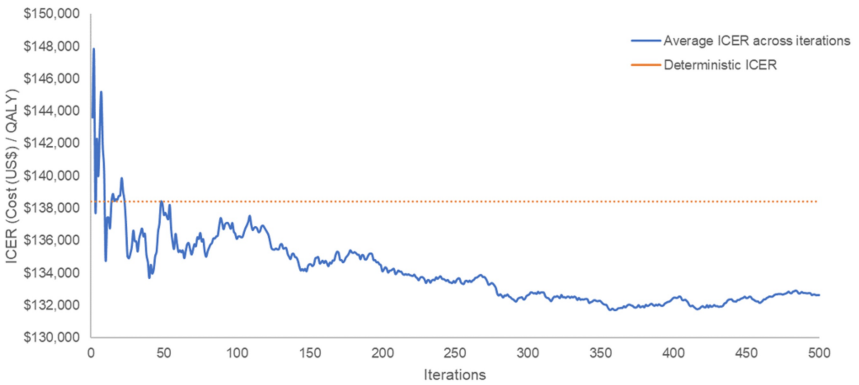


FIGURE 6: ICER convergence plots

PSMA, prostate-specific membrane antigen; ICER, incremental cost-effectiveness ratio; QALY, quality-adjusted life year.

Figure created by the authors using Microsoft Excel (Redmond, WA, USA).

The results were consistent with the base case findings, with piflufolastat F 18 emerging as the most effective strategy, yielding the highest LYs (6.82) and QALYs (5.35). It also demonstrated the greatest NMB at $619,594 when compared to other imaging modalities (Table 6).

Diagnostic options	Total			Incremental outcomes (Piflufolastat F 18 – each comparator)			Combined outcomes		
	Cost ($)	LY	QALY	Δ Cost ($)	Δ LY	Δ QALY	ICER ($/LY)	ICER ($/QALY)	Net monetary benefit (WTP threshold of $150,000)
Piflufolastat F 18	182,556	6.82	5.348	-	-	-	-	-	619,594
Flotufolastat F 18	182,158	6.52	5.031	398	0.3012	0.317	1,322	1,256	572,444
PSMA 11	179,656	6.78	5.316	2,900	0.04	0.032	72,583	90,512	617,688
Conventional imaging (MRI, SPECT, CT equally weighted)	154,263	6.6	5.134	28,293	0.2192	0.2133	129,103	132,653	615,895

TABLE 6: Probabilistic sensitivity analysis results

Costs are presented in 2023 United States dollars. Abbreviations: PSMA, prostate-specific membrane antigen; CT, computed tomography; ICER, incremental cost-effectiveness ratio; LY, life year; MRI, magnetic resonance imaging; PSMA 11, gallium Ga68 PSMA-11; QALY, quality-adjusted life year; SPECT, single-photon emission computerized tomography; WTP, willingness to pay.

On the cost-effectiveness plane, comparisons of piflufolastat F 18 against flotufolastat F 18 and PSMA 11 placed the ICER in the northeast quadrant in the majority of simulations (Figure 7). The ICER was under the $150,000 WTP threshold in all simulations when compared to flotufolastat F 18, as well as in the majority of simulations when compared to PSMA 11. When compared to flotufolastat F 18, incremental QALYs were consistently above zero, though there were some uncertainties in incremental costs (i.e., simulated values were on both the positive and negative sides of the cost axis). For PSMA 11, there were uncertainties in both incremental costs and QALYs. At a WTP threshold of $150,000, there was a 100% probability that piflufolastat F 18 is cost-effective when compared to flotufolastat F 18, and a 78.4% probability when compared to PSMA 11.

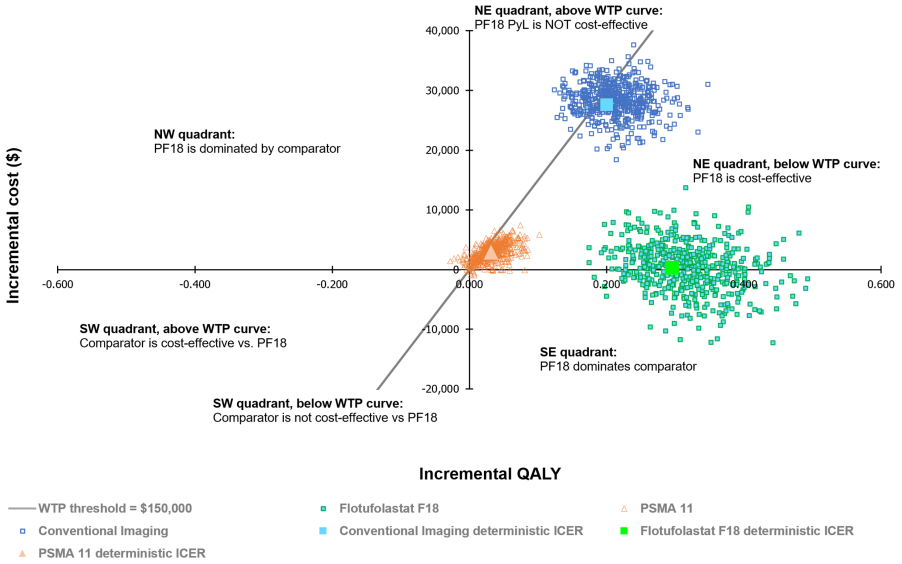


FIGURE 7: Cost-effectiveness plane for piflufolastat F 18 relative to comparator imaging strategies.

All costs are reported in 2023 US dollars. Abbreviations: PSMA, prostate-specific membrane antigen; ICER, incremental cost-effectiveness ratio; NE, northeast; NW, northwest; PF18, piflufolastat F 18; PSMA 11, gallium Ga68 PSMA-11; SE, southeast; SW, southwest; QALY, quality-adjusted life year; WTP, willingness to pay.

Figure created by the authors using Microsoft Excel (Redmond, WA, USA).

On the cost-effectiveness plane comparing piflufolastat F 18 with CI, piflufolastat F 18 was associated with higher costs across all probabilistic simulations, while the majority of simulations also demonstrated greater health gains. At a WTP threshold of $150,000 per QALY gained, piflufolastat F 18 had a 71.0% probability of being the cost-effective strategy relative to CI.

Across all imaging strategies evaluated, piflufolastat F 18 had the highest probability of being the optimal cost-effective option (57.8%), followed by CI (27.8%), PSMA 11 (14.4%), and flotufolastat F 18 (0.0%) (Figure *8*).

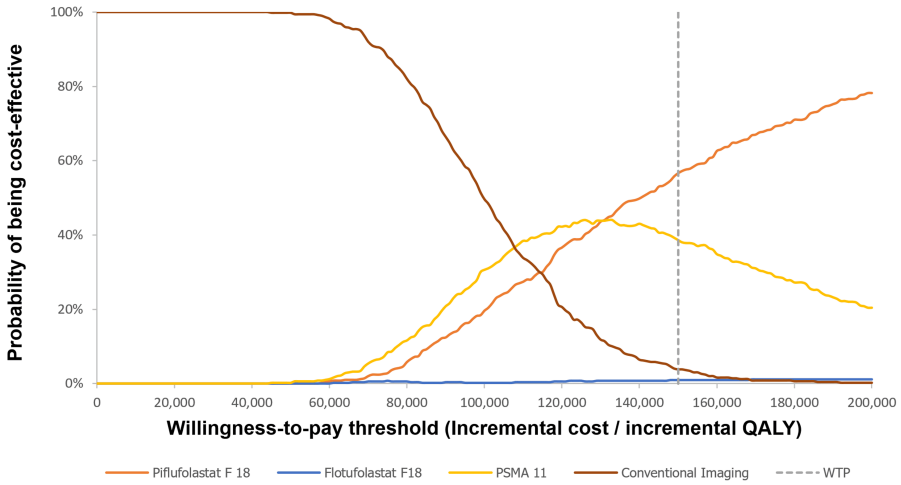


FIGURE 8: Cost-effectiveness acceptability curve (combined)

WTP thresholds are in 2023 United States dollars. Abbreviations: PSMA, prostate-specific membrane antigen; PSMA 11, gallium Ga68 PSMA-11; QALY, quality-adjusted life year; WTP, willingness to pay.

Figure created by the authors using Microsoft Excel (Redmond, WA, USA).

Discussion

The introduction of novel PSMA PET radiotracers has provided new options for the detection and characterization of prostate cancer with greater sensitivity and specificity, although it is important to understand their relative cost-effectiveness to optimize both healthcare resource allocation and decision-making. The results of the present analysis indicate that piflufolastat F 18 is associated with favorable cost-effective outcomes compared to alternative PSMA PET agents, including flotufolastat F 18, in the evaluation of prostate cancer. In the base case model, piflufolastat F 18 led to more total LYs and QALYs along with a greater NMB relative to comparators, despite having higher total costs. The results of the DSA showed the sensitivity of the results to the costs and detection sensitivity of the imaging agents, the probability of cure with the assigned treatment, disease distribution, and the utility of different health states. Consistent with the base case results, the probabilistic sensitivity analysis demonstrated that piflufolastat F 18 had a 100% probability of being cost-effective compared to flotufolastat F 18, at a WTP threshold of $150,000 per QALY gained. Piflufolastat F 18 also showed a high probability of being more cost-effective than PSMA 11 (78.4%) and CI (71.0%).

The probabilistic sensitivity analysis indicated that the results were most sensitive to variation in imaging costs, diagnostic sensitivity, the distribution of regional and metastatic disease, baseline PSA distributions, and utility estimates associated with disease-free and localized disease states. Although the comparison between piflufolastat F 18 and PSMA 11 exhibited greater uncertainty than the comparisons with flotufolastat F 18 or CI, largely because of uncertainty surrounding the incremental QALY estimates, piflufolastat F 18 remained more likely to be the more cost-effective strategy. At a willingness-to-pay threshold of $150,000 per QALY gained, the probability that piflufolastat F 18 would be cost-effective relative to PSMA 11 was 78%. This finding appears to be attributable to the higher sensitivity estimates across both PSA levels and the higher specificity estimate for patients with PSA ⩽ 1.0 associated with piflufolastat F 18 in the evidence sources used for the model, despite both agents targeting PSMA. Overall, the analysis suggests that piflufolastat F 18 offers favorable cost-effectiveness compared with conventional imaging in prostate cancer, and the conclusions remained generally consistent across a broad range of deterministic and probabilistic sensitivity analyses.

As shown in the present analysis, PSMA PET-based imaging strategies generally incur higher upfront diagnostic costs than conventional modalities such as MRI, CT, or SPECT. However, these additional costs

may be offset by improvements in diagnostic accuracy, which can translate into improved clinical outcomes and more favorable cost-effectiveness. Current prostate cancer management guidelines recognize PSMA PET as an effective imaging modality and recommend its use in settings where it may reduce the need for additional imaging during initial staging or following BCR [16,18,21,37]. Consistent with these recommendations, evidence from several international studies has suggested that newer PET radiotracers may offer both economic and clinical advantages over conventional imaging approaches.

For instance, an Australian cost-effectiveness analysis compared PSMA 11 PET/MRI with standard imaging (MRI, bone scintigraphy) in patients with BCR using data from a prospective single-center study [76]. Over a 10-year time horizon, the PSMA 11 strategy was projected to yield 7.48 life-years compared with 7.41 life-years for standard care, for a reduced cost (56,961 vs. 64,499 AUD), representing a cost-saving alternative. In probabilistic sensitivity analyses, it demonstrated a substantially greater probability of being considered cost-effective at commonly applied willingness-to-pay thresholds, although QALYs were not evaluated. Another analysis conducted in European and US settings concluded that, despite the higher acquisition costs associated with PSMA PET/CT, the value of improved diagnostic accuracy outweighed the consequences and costs associated with diagnostic misclassification [77]. Similarly, an Australian evaluation comparing PSMA PET/CT with CT plus whole-body bone scanning found that PSMA PET/CT had a high probability of representing a cost-effective strategy at a willingness-to-pay threshold of AUD $50,000 per QALY gained [78]. In addition, a French economic evaluation of imaging approaches for detecting bone metastases after BCR reported that 18F-choline PET offered more favorable cost-effectiveness outcomes than conventional MRI and PET-based alternatives [79].

This study has several important strengths. Notably, the model captures a comprehensive diagnostic and treatment pathway spanning from initial diagnosis through BCR, a feature that is not commonly incorporated in previously published prostate cancer cost-effectiveness analyses [76,79,80]. The evaluation also considered a broad range of diagnostic imaging strategies and accounted for variation in test performance by incorporating PSA-stratified sensitivity and specificity estimates [19,81]. This approach helped ensure that differences in diagnostic accuracy reflected underlying PSA levels rather than being attributed solely to the imaging modalities themselves. In addition, the model included multiple treatment options together with the costs and quality-of-life decrements associated with treatment-related adverse events. As a result, the analysis was able to quantify the economic and clinical value of improved treatment selection, including the avoidance of unnecessary interventions among patients unlikely to derive meaningful benefit.

The findings of the present analysis are consistent with and extend those reported in our previous cost-effectiveness evaluation of piflufolastat F 18 [39], and collectively demonstrate that piflufolastat F 18 is more cost-effective than CI as well as alternative PET tracers PSMA 11, fluciclovine F 18, and flotufolastat F 18 at initial diagnosis and BCR. Results from both modeling studies suggest that the use of PSMA PET imaging may confer sustained long-term clinical and economic benefits. These projections should be reassessed as longer-term real-world evidence becomes available and the adoption of PSMA PET tracers for primary staging and recurrence assessment continues to expand. Enhancing diagnostic accuracy remains a critical component of prostate cancer management, as more precise imaging can support better-informed treatment selection and ultimately improve patient outcomes.

Limitations

Several limitations should be considered when interpreting the findings of this study. First, estimates of diagnostic performance for piflufolastat F 18 and the distributions of disease stage and PSA levels among patients with prostate cancer were derived from the OSPREY (NCT02981368) and CONDOR (NCT03739684) trials, whereas corresponding estimates for flotufolastat F 18 came from the LIGHTHOUSE (NCT04186819) trial [82-84]. As a result, these inputs may not fully reflect outcomes observed in routine clinical practice among a more general patient population. However, sensitivity analyses demonstrated that variation in these parameters had a limited impact on the overall conclusion, with ICERs staying within the WTP threshold across most scenarios.

Second, treatment decisions following diagnosis were informed by assumptions about disease states. Reliable estimates of treatment patterns by disease state were difficult to obtain in the absence of detailed analyses of claims or medical record data. To address this evidence gap, interviews were conducted with US-based oncologists experienced in the management of prostate cancer.

Third, the model assumed that BCR could occur only once during a patient's lifetime, whereas repeated recurrences may occur in real-world clinical practice, which would lead to additional costs for these patients. However, if repeat BCR occurs at similar rates across imaging strategies, the additional costs and QALY decrements would be broadly comparable between them. Fourth, chemotherapy was not included among first-line treatment options either at initial diagnosis or at BCR. Fifth, diagnostic accuracy estimates for some comparators were obtained from different studies, relying on individual study arms. As a result, comparisons of sensitivity and specificity across modalities were indirect and may have been influenced by differences in study populations or other unmeasured factors. In addition, diagnostic performance inputs were stratified according to PSA level rather than disease extent (localized, regional, or metastatic). Sixth,

the assumption of no additional imaging or diagnostic costs following an incorrect diagnosis does not account for the likelihood that a patient having a false negative would incur these costs upon re-evaluation following clinical progression. Seventh, the assumption that an incorrect diagnosis based on a false positive or false negative test result would inform the subsequent treatment assignment may not be fully reflective of real-world clinical practice, where additional work-up may be performed to inform clinical management. Eighth, the cost inputs for the model are meant to reflect an average cost across all insurance payers, but may not reflect the differences between individual payers in the real world. This was partially addressed by the DSA analyses, which sought to evaluate the uncertainty in diagnostic costs.

Ninth, a previously published systematic review and meta-analysis reported diagnostic accuracy estimates that differ from those used in the present model, additionally suggesting that radiotracer selection may not substantially affect test performance. The same study also reported different cost-effectiveness results when comparing PSMA PET/CT to CI [41,78]. In contrast, the current analysis relied on evidence identified through a targeted literature review, which is inherently narrower in scope than a systematic review and meta-analysis. Differences in reported ICERs may partly be explained by variation in the relative costs of PSMA PET/CT and CI in Australia versus the US, but this remains a limitation of the current study regardless. Finally, the analysis did not consider potential future changes in diagnostic or treatment costs.

Conclusions

The findings from this analysis suggest that piflufolastat F 18 offers a cost-effective imaging strategy for patients with prostate cancer in the US. Compared with flotufolastat F 18, PSMA 11, and CI, piflufolastat F 18 was associated with higher incremental LYs and QALYs, along with a greater net monetary benefit. These results provide evidence that may support healthcare decision-makers in evaluating the clinical and economic implications of adopting piflufolastat F 18 for the diagnosis and staging of prostate cancer.

Additional Information

Author Contributions

All authors have reviewed the final version to be published and agreed to be accountable for all aspects of the work.

Concept and design: Christopher W. Yee, Noam Kirson, Christopher Tyson

Acquisition, analysis, or interpretation of data: Christopher W. Yee, Noam Kirson, Yiqiao Xin, Christopher Tyson, Mitchell Finkelstein, Steven E. Finkelstein

Drafting of the manuscript: Christopher W. Yee, Noam Kirson, Yiqiao Xin

Critical review of the manuscript for important intellectual content: Christopher W. Yee, Noam Kirson, Yiqiao Xin, Christopher Tyson, Mitchell Finkelstein, Steven E. Finkelstein

Supervision: Christopher W. Yee, Noam Kirson

Disclosures

Human subjects: Informed consent for treatment and open access publication was obtained or waived by all participants in this study. **Animal subjects:** All authors have confirmed that this study did not involve animal subjects or tissue. **Conflicts of interest:** In compliance with the ICMJE uniform disclosure form, all authors declare the following: **Payment/services info:** Christopher Yee, Yiqiao Xin, and Noam Kirson are employees of Analysis Group, Inc., which has received consulting fees from Lantheus. Christopher Tyson is an employee of Lantheus. **Financial relationships:** All authors have declared that they have no financial relationships at present or within the previous three years with any organizations that might have an interest in the submitted work. **Other relationships:** All authors have declared that there are no other relationships or activities that could appear to have influenced the submitted work.

Acknowledgements

The authors thank Dr. Daniel Lin, MD, of the University of Washington School of Medicine; Dr. Edward Schaeffer, MD, PhD, of Northwestern University; Dr. Eric Klein, MD, of the Cleveland Clinic; Dr. Soroush Rais-Bahrami, MD, MBA, of the University of Alabama at Birmingham; and Dr. Bela Denes, MD, of Lantheus, for providing their helpful insights on clinical inputs and study design. Medical writing was provided by Shelley Batts, PhD, an independent contractor of Analysis Group, Inc., and funded by Lantheus.

References

1. James ND, Tannock I, N'Dow J, et al.: The Lancet Commission on prostate cancer: planning for the surge in cases. Lancet. 2024, 403:1683-722. 10.1016/S0140-6736(24)00651-2
2. Sung H, Ferlay J, Siegel RL, Laversanne M, Soerjomataram I, Jemal A, Bray F: Global cancer statistics 2020:

GLOBOCAN estimates of incidence and mortality worldwide for 36 cancers in 185 countries. CA Cancer J Clin. 2021, 71:209-49. 10.3322/caac.21660
3. Cancer stat facts: prostate cancer. (2026). Accessed: April 26, 2026: https://seer.cancer.gov/statfacts/html/prost.html.
4. Siegel RL, Giaquinto AN, Jemal A: Cancer statistics, 2024. CA Cancer J Clin. 2024, 74:12-49. 10.3322/caac.21820
5. Cancer statistics, 2024. (2024). Accessed: December 11, 2024: https://www.cancer.org/research/cancer-facts-statistics/all-cancer-facts-figures/2024-cancer-facts-figures.html.
6. Grossman DC, Curry SJ, Owens DK, et al.: Screening for prostate cancer: US Preventive Services Task Force recommendation statement. JAMA. 2018, 319:1901-13. 10.1001/jama.2018.3710
7. Wolf AM, Wender RC, Etzioni RB, et al.: American Cancer Society guideline for the early detection of prostate cancer: update 2010. CA Cancer J Clin. 2010, 60:70-98. 10.3322/caac.20066
8. Carter HB, Albertsen PC, Barry MJ, et al.: Early detection of prostate cancer: AUA guideline . J Urol. 2013, 190:419-26. 10.1016/j.juro.2013.04.119
9. Wei JT, Barocas D, Carlsson S, et al.: Early detection of prostate cancer: AUA/SUO guideline part I: prostate cancer screening. J Urol. 2023, 210:46-53. 10.1097/JU.0000000000003491
10. Initial treatment of prostate cancer, by stage and risk group . (2026). Accessed: April 26, 2026: https://www.cancer.org/cancer/types/prostate-cancer/treating/by-stage.html.
11. Artibani W, Porcaro AB, De Marco V, Cerruto MA, Siracusano S: Management of biochemical recurrence after primary curative treatment for prostate cancer: a review. Urol Int. 2018, 100:251-62. 10.1159/000481438
12. Briganti A, Joniau S, Gandaglia G, et al.: Patterns and predictors of early biochemical recurrence after radical prostatectomy and adjuvant radiation therapy in men with pT3N0 prostate cancer: implications for multimodal therapies. Int J Radiat Oncol Biol Phys. 2013, 87:960-7. 10.1016/j.ijrobp.2013.09.015
13. Rebello RJ, Oing C, Knudsen KE, et al.: Prostate cancer. Nat Rev Dis Primers. 2021, 7:9. 10.1038/s41572-020-00243-0
14. Diagnosing prostate cancer. (2026). Accessed: April 26, 2026: https://www.cdc.gov/prostate-cancer/diagnosis/index.html.
15. Trabulsi EJ, Rumble RB, Jadvar H, et al.: Optimum imaging strategies for advanced prostate cancer: ASCO guideline. J Clin Oncol. 2020, 38:1963-96. 10.1200/JCO.19.02757
16. Eastham JA, Auffenberg GB, Barocas DA, et al.: Clinically localized prostate cancer: AUA/ASTRO guideline, Part I: Introduction, risk assessment, staging, and risk-based management. J Urol. 2022, 208:10-8. 10.1097/JU.0000000000002757
17. Bednarova S, Lindenberg ML, Vinsensia M, Zuiani C, Choyke PL, Turkbey B: Positron emission tomography (PET) in primary prostate cancer staging and risk assessment. Transl Androl Urol. 2017, 6:413-23. 10.21037/tau.2017.03.53
18. Eastham JA, Auffenberg GB, Barocas DA, et al.: Clinically localized prostate cancer: AUA/ASTRO guideline, Part II: Principles of active surveillance, principles of surgery, and follow-Up. J Urol. 2022, 208:19-25. 10.1097/JU.0000000000002758
19. Fendler WP, Calais J, Eiber M, et al.: Assessment of 68Ga-PSMA-11 PET accuracy in localizing recurrent prostate cancer: a prospective single-arm clinical trial. JAMA Oncol. 2019, 5:856-63. 10.1001/jamaoncol.2019.0096
20. De Visschere PJ, Standaert C, Fütterer JJ, et al.: A systematic review on the role of imaging in early recurrent prostate cancer. Eur Urol Oncol. 2019, 2:47-76. 10.1016/j.euo.2018.09.010
21. Lowrance WT, Breau RH, Chou R, et al.: Advanced prostate cancer: AUA/ASTRO/SUO guideline part II . J Urol. 2021, 205:22-9. 10.1097/JU.0000000000001376
22. Meijer D, Eppinga WS, Mohede RM, et al.: Prostate-specific membrane antigen positron emission tomography/computed tomography is associated with improved oncological outcome in men treated with salvage radiation therapy for biochemically recurrent prostate cancer. Eur Urol Oncol. 2022, 5:146-52. 10.1016/j.euo.2022.01.001
23. Silver DA, Pellicer I, Fair WR, Heston WD, Cordon-Cardo C: Prostate-specific membrane antigen expression in normal and malignant human tissues. Clin Cancer Res. 1997, 3:81-5.
24. Bostwick DG, Pacelli A, Blute M, Roche P, Murphy GP: Prostate specific membrane antigen expression in prostatic intraepithelial neoplasia and adenocarcinoma: a study of 184 cases. Cancer. 1998, 82:2256-61. 10.1002/(sici)1097-0142(19980601)82:11<2256::aid-cncr22>3.0.co;2-s
25. Maurer T, Eiber M, Schwaiger M, Gschwend JE: Current use of PSMA-PET in prostate cancer management . Nat Rev Urol. 2016, 13:226-35. 10.1038/nrurol.2016.26
26. Donin NM, Reiter RE: Why targeting PSMA is a game changer in the management of prostate cancer . J Nucl Med. 2018, 59:177-82. 10.2967/jnumed.117.191874
27. Bluemel C, Krebs M, Polat B, et al.: 68Ga-PSMA-PET/CT in patients with biochemical prostate cancer recurrence and negative 18F-choline-PET/CT. Clin Nucl Med. 2016, 41:515-21. 10.1097/RLU.0000000000001197
28. Hofman MS, Lawrentschuk N, Francis RJ, et al.: Prostate-specific membrane antigen PET-CT in patients with high-risk prostate cancer before curative-intent surgery or radiotherapy (proPSMA): a prospective, randomised, multicentre study. Lancet. 2020, 395:1208-16. 10.1016/S0140-6736(20)30314-7
29. Ng M, Guerrieri M, Wong LM, et al.: Changes in management after (18)F-DCFPYL PSMA PET in patients undergoing postprostatectomy radiotherapy, with early biochemical response outcomes. J Nucl Med. 2022, 63:1343-8. 10.2967/jnumed.121.263521
30. Morris MJ, Rowe SP, Gorin MA, et al.: Diagnostic performance of (18)F-DCFPyL-PET/CT in men with biochemically recurrent prostate cancer: results from the the CONDOR Phase III, multicenter study. Clin Cancer Res. 2021, 27:3674-82. 10.1158/1078-0432.CCR-20-4573
31. Rousseau E, Wilson D, Lacroix-Poisson F, et al.: A prospective study on (18)F-DCFPyL PSMA PET/CT imaging in biochemical recurrence of prostate cancer. J Nucl Med. 2019, 60:1587-93. 10.2967/jnumed.119.226381

32. Mena E, Lindenberg L, Choyke PL: Update on PSMA-based prostate cancer imaging . Semin Nucl Med. 2024, 54:941-50. 10.1053/j.semnuclmed.2024.10.004
33. Prescribing information for Gallium Ga 68 PSMA-11 . (2020). Accessed: December 11, 2024: https://www.accessdata.fda.gov/drugsatfda_docs/label/2020/212642s000lbl.pdf.
34. Prescribing information for PYLARIFY (piflufolastat F 18) . (2021). Accessed: December 11, 2024: https://www.accessdata.fda.gov/drugsatfda_docs/label/2021/214793s000lbl.pdf.
35. Prescribing information for POSLUMA (flotufolastat F 18). (2023). Accessed: December 11, 2024: https://www.accessdata.fda.gov/drugsatfda_docs/label/2023/216023s000lbl.pdf.
36. Prescribing information for AXUMIN (fluciclovine F 18) . (2016). Accessed: December 11, 2024: https://www.accessdata.fda.gov/drugsatfda_docs/label/2016/208054s000lbl.pdf.
37. Lowrance WT, Breau RH, Chou R, et al.: Advanced prostate cancer: AUA/ASTRO/SUO guideline part I . J Urol. 2021, 205:14-21. 10.1097/JU.0000000000001375
38. Armstrong AJ, Morris MJ, Abida W, et al.: Trial design and objectives for patients with prostate cancer: recommendations from the Prostate Cancer Working Group 4. J Clin Oncol. 2026, 44:1249-65. 10.1200/JCO-25-02834
39. Yee CW, Harvey MJ, Xin Y, Kirson NY: Cost-effectiveness modeling of prostate-specific membrane antigen positron emission tomography with piflufolastat F 18 for the initial diagnosis of patients with prostate cancer in the United States. Pharmacoeconomics. 2024, 42:231-47. 10.1007/s40273-023-01322-2
40. Surasi DS, Eiber M, Maurer T, et al.: Diagnostic performance and safety of positron emission tomography with (18)F-rhPSMA-7.3 in patients with newly diagnosed unfavourable intermediate- to very-high-risk prostate cancer: results from a Phase 3, prospective, multicentre study (LIGHTHOUSE). Eur Urol. 2023, 84:361-70. 10.1016/j.eururo.2023.06.018
41. Jeet V, Parkinson B, Song R, Sharma R, Hoyle M: Histopathologically validated diagnostic accuracy of PSMA-PET/CT in the primary and secondary staging of prostate cancer and the impact of PSMA-PET/CT on clinical management: a systematic review and meta-analysis. Semin Nucl Med. 2023, 53:706-18. 10.1053/j.semnuclmed.2023.02.006
42. Clinical study report: PyL-2301 (Data on File) . Progenics Pharmaceuticals, Bedford; 2020.
43. Clinical study report: PyL-3301 (Data on File) . Progenics Pharmaceuticals, Bedford; 2020.
44. Jensen IS, Hathway J, Cyr P, Gauden D, Gardiner P: Cost-consequence analysis of (18)F-fluciclovine for the staging of recurrent prostate cancer. J Mark Access Health Policy. 2020, 8:1749362. 10.1080/20016689.2020.1749362
45. Andriole GL, Kostakoglu L, Chau A, et al.: The impact of positron emission tomography with 18F-fluciclovine on the treatment of biochemical recurrence of prostate cancer: results from the LOCATE trial. J Urol. 2019, 201:322-31. 10.1016/j.juro.2018.08.050
46. Physician fee schedule. (2020). Accessed: December 14, 2020: https://www.cms.gov/apps/physician-fee-schedule/search/search-criteria.aspx.
47. RED BOOK online. (2022). Accessed: August 20, 2022: https://www.micromedexsolutions.com/.
48. Cowen ME, Chartrand M, Weitzel WF: A Markov model of the natural history of prostate cancer . J Clin Epidemiol. 1994, 47:3-21. 10.1016/0895-4356(94)90029-9
49. de Koning HJ, Auvinen A, Berenguer Sanchez A, et al.: Large-scale randomized prostate cancer screening trials: program performances in the European Randomized Screening for Prostate Cancer trial and the Prostate, Lung, Colorectal and Ovary cancer trial. Int J Cancer. 2002, 97:237-44. 10.1002/ijc.1588
50. de Koning HJ, Liem MK, Baan CA, Boer R, Schröder FH, Alexander FE: Prostate cancer mortality reduction by screening: power and time frame with complete enrollment in the European Randomised Screening for Prostate Cancer (ERSPC) trial. Int J Cancer. 2002, 98:268-73. 10.1002/ijc.10188
51. Draisma G, Boer R, Otto SJ, van der Cruijsen IW, Damhuis RA, Schröder FH, de Koning HJ: Lead times and overdetection due to prostate-specific antigen screening: estimates from the European Randomized Study of Screening for Prostate Cancer. J Natl Cancer Inst. 2003, 95:868-78. 10.1093/jnci/95.12.868
52. Young JL Jr, Percy CL, Asire AJ, et al.: Cancer incidence and mortality in the United States, 1973-77 . Natl Cancer Inst Monogr. 1981, 1-187.
53. Cooperberg MR, Ramakrishna NR, Duff SB, Hughes KE, Sadownik S, Smith JA, Tewari AK: Primary treatments for clinically localised prostate cancer: a comprehensive lifetime cost-utility analysis. BJU Int. 2013, 111:437-50. 10.1111/j.1464-410X.2012.11597.x
54. Sciarra A, Fasulo A, Ciardi A, et al.: A meta-analysis and systematic review of randomized controlled trials with degarelix versus gonadotropin-releasing hormone agonists for advanced prostate cancer. Medicine (Baltimore). 2016, 95:e3845. 10.1097/MD.0000000000003845
55. Zhou JT, Fang DM, Xia S, Li T, Liu RL: The incidence proportion of erectile dysfunction in patients treated with cryotherapy for prostate cancer: a meta-analysis. Clin Transl Oncol. 2019, 21:1152-8. 10.1007/s12094-019-02036-8
56. Roberts CB, Jang TL, Shao YH, Kabadi S, Moore DF, Lu-Yao GL: Treatment profile and complications associated with cryotherapy for localized prostate cancer: a population-based study. Prostate Cancer Prostatic Dis. 2011, 14:313-9. 10.1038/pcan.2011.17
57. Trock BJ, Han M, Freedland SJ, Humphreys EB, DeWeese TL, Partin AW, Walsh PC: Prostate cancer-specific survival following salvage radiotherapy vs observation in men with biochemical recurrence after radical prostatectomy. JAMA. 2008, 299:2760-9. 10.1001/jama.299.23.2760
58. Bauman G, Ding K, Chin J, et al.: Cryosurgery versus primary androgen deprivation therapy for locally recurrent prostate cancer after primary radiotherapy: a propensity-matched survival analysis. Cureus. 2020, 12:e7983. 10.7759/cureus.7983
59. Chade DC, Shariat SF, Cronin AM, et al.: Salvage radical prostatectomy for radiation-recurrent prostate cancer: a multi-institutional collaboration. Eur Urol. 2011, 60:205-10. 10.1016/j.eururo.2011.03.011
60. Appukkuttan S, Tangirala K, Babajanyan S, Wen L, Simmons S, Shore N: A retrospective claims analysis of advanced prostate cancer costs and resource use. Pharmacoecon Open. 2020, 4:439-47. 10.1007/s41669-019-00185-8
61. Tangirala K, Appukkuttan S, Simmons S: Costs and healthcare resource utilization associated with hospital

admissions of patients with metastatic or nonmetastatic prostate cancer. Am Health Drug Benefits. 2019, 12:306-12.
62. Jiang R, Janssen MF, Pickard AS: US population norms for the EQ-5D-5L and comparison of norms from face-to-face and online samples. Qual Life Res. 2021, 30:803-16. 10.1007/s11136-020-02650-y
63. Stewart ST, Lenert L, Bhatnagar V, Kaplan RM: Utilities for prostate cancer health states in men aged 60 and older. Med Care. 2005, 43:347-55. 10.1097/01.mlr.0000156862.33341.45
64. NDA 216023 / Flotufolastat F 18 (Posluma): multi-disciplinary review and evaluation . (2022). Accessed: April 26, 2026: https://www.accessdata.fda.gov/drugsatfda_docs/nda/2023/216023Orig1s000MultidisciplineR.pdf.
65. Asokendaran ME, Meyrick DP, Skelly LA, Lenzo NP, Henderson A: Gallium-68 prostate-specific membrane antigen positron emission tomography/computed tomography compared with diagnostic computed tomography in relapsed prostate cancer. World J Nucl Med. 2019, 18:232-7. 10.4103/wjnm.WJNM_59_18
66. de Leiris N, Leenhardt J, Boussat B, et al.: Does whole-body bone SPECT/CT provide additional diagnostic information over [18F]-FCH PET/CT for the detection of bone metastases in the setting of prostate cancer biochemical recurrence?. Cancer Imaging. 2020, 20:58. 10.1186/s40644-020-00333-y
67. Li Y, Han D, Wu P, et al.: Comparison of (68)Ga-PSMA-617 PET/CT with mpMRI for the detection of PCa in patients with a PSA level of 4-20 ng/ml before the initial biopsy. Sci Rep. 2020, 10:10963. 10.1038/s41598-020-67385-9
68. Scarsbrook AF, Bottomley D, Teoh EJ, et al.: Effect of (18)f-fluciclovine positron emission tomography on the management of patients with recurrence of prostate cancer: results from the FALCON trial. Int J Radiat Oncol Biol Phys. 2020, 107:316-24. 10.1016/j.ijrobp.2020.01.050
69. Bach-Gansmo T, Nanni C, Nieh PT, et al.: Multisite experience of the safety, detection rate and diagnostic performance of Fluciclovine ((18)f) positron emission tomography/computerized tomography imaging in the staging of biochemically recurrent prostate cancer. J Urol. 2017, 197:676-83. 10.1016/j.juro.2016.09.117
70. Research data assistance center (ResDac). (2018). Accessed: August 21, 2018: https://www.resdac.org/.
71. Consumer price index for all urban consumers, not seasonally adjusted: U.S. city average for medical care, 2000-2020. (2020). http://download.bls.gov/pub/time.series/cu/cu.data.15.USMedical.
72. Haacker M, Hallett TB, Atun R: On discount rates for economic evaluations in global health . Health Policy Plan. 2020, 35:107-14. 10.1093/heapol/czz127
73. The cost-effectiveness analysis registry. (2021). Accessed: June 30, 2021: https://cear.tuftsmedicalcenter.org/.
74. 2020-2023 Value Assessment Framework. Institute for Clinical and Economic Review, Boston; 2020.
75. Husereau D, Drummond M, Augustovski F, et al.: Consolidated Health Economic Evaluation Reporting Standards 2022 (CHEERS 2022) statement: updated reporting guidance for health economic evaluations. Value Health. 2022, 25:3-9. 10.1016/j.jval.2021.11.1351
76. Gordon LG, Elliott TM, Joshi A, Williams ED, Vela I: Exploratory cost-effectiveness analysis of (68)Gallium-PSMA PET/MRI-based imaging in patients with biochemical recurrence of prostate cancer. Clin Exp Metastasis. 2020, 37:305-12. 10.1007/s10585-020-10027-1
77. Holzgreve A, Unterrainer M, Calais J, et al.: Is PSMA PET/CT cost-effective for the primary staging in prostate cancer? First results for European countries and the USA based on the proPSMA trial. Eur J Nucl Med Mol Imaging. 2023, 50:3750-4. 10.1007/s00259-023-06332-y
78. Song R, Jeet V, Sharma R, Hoyle M, Parkinson B: Cost-effectiveness analysis of prostate-specific membrane antigen (PSMA) positron emission tomography/computed tomography (PET/CT) for the primary staging of prostate cancer in Australia. Pharmacoeconomics. 2022, 40:807-21. 10.1007/s40273-022-01156-4
79. Gauthé M, Zarca K, Aveline C, et al.: Comparison of (18)F-sodium fluoride PET/CT, (18)F-fluorocholine PET/CT and diffusion-weighted MRI for the detection of bone metastases in recurrent prostate cancer: a cost-effectiveness analysis in France. BMC Med Imaging. 2020, 20:25. 10.1186/s12880-020-00425-y
80. Keeney E, Thom H, Turner E, Martin RM, Morley J, Sanghera S: Systematic review of cost-effectiveness models in prostate cancer: exploring new developments in testing and diagnosis. Value Health. 2022, 25:133-46. 10.1016/j.jval.2021.07.002
81. Hoffmann MA, Buchholz HG, Wieler HJ, et al.: PSA and PSA kinetics thresholds for the presence of (68)Ga-PSMA-11 PET/CT-detectable lesions in patients with biochemical recurrent prostate cancer. Cancers (Basel). 2020, 12:10.3390/cancers12020398
82. Study of 18F-DCFPyL PET/CT imaging in patients with prostate cancer (OSPREY) . (2021). Accessed: September 22, 2026: https://clinicaltrials.gov/study/NCT02981368.
83. Study of 18F-DCFPyL PET/CT imaging in patients with suspected recurrence of prostate cancer (CONDOR) . (2021). Accessed: September 22, 2026: https://clinicaltrials.gov/study/NCT03739684.
84. Imaging study to investigate the safety and diagnostic performance of rhPSMA 7.3 (18F) in newly diagnosed prostate cancer. (2025). Accessed: September 22, 2026: https://clinicaltrials.gov/study/NCT04186819.